




Quantitative Electroencephalography in Term Neonates During the Early Postnatal Period Across Various Sleep States

Ruijie Zhang^{1,*}, Xinran Dong^{2,*}, Lu Zhang^{1,*}, Xinao Lin¹ , Xuefeng Wang¹, Yan Xu³, Chuyan Wu⁴ , Feng Jiang¹ , Jimei Wang¹

¹Department of Neonatology, Obstetrics and Gynecology Hospital of Fudan University, Shanghai, People's Republic of China; ²Center for Molecular Medicine, Children's Hospital of Fudan University, Shanghai, People's Republic of China; ³Department of Neurology, Children's Hospital of Fudan University, National Children's Medical Center, Shanghai, People's Republic of China; ⁴Department of Rehabilitation Medicine, The First Affiliated Hospital of Nanjing Medical University, Nanjing, People's Republic of China

*These authors contributed equally to this work

Correspondence: Jimei Wang; Feng Jiang, Department of Neonatology, Obstetrics and Gynecology Hospital of Fudan University, Shanghai, 200011, People's Republic of China, Email wjm821920@163.com; dxyjiang@163.com

Background: Neonatal sleep is pivotal for their growth and development, yet manual interpretation of raw images is time-consuming and labor-intensive. Quantitative Electroencephalography (QEEG) presents significant advantages in terms of objectivity and convenience for investigating neonatal sleep patterns. However, research on the sleep patterns of healthy neonates remains scarce. This study aims to identify QEEG markers that distinguish between different neonatal sleep cycles and analyze QEEG alterations across various sleep stages in relation to postmenstrual age.

Methods: From September 2023 to February 2024, full-term neonates admitted to the neonatology department at the Obstetrics and Gynecology Hospital of Fudan University were enrolled in this study. Electroencephalographic (EEG) recordings were obtained from neonates aged 37–42 weeks, within 1–7 days post-birth. The ROC curve was employed to evaluate QEEG features related to amplitude, range EEG (rEEG), spectral density, and connectivity across different sleep stages. Furthermore, regression analyses were performed to investigate the association between these QEEG characteristics and postmenstrual age.

Results: The alpha frequency band's spectral_diff_F3 emerged as the most potent discriminator between active sleep (AS) and quiet sleep (QS). In distinguishing AS from wakefulness (W), the theta frequency's spectral_diff_C4 was the most effective, whereas the delta frequency's spectral_diff_P4 excelled in differentiating QS from W. During AS and QS phases, there was a notable increase in entropy within the delta frequency band across all monitored brain regions and in the spectral relative power within the theta frequency band, correlating with postmenstrual age (PMA).

Conclusion: Spectral difference showcases the highest discriminative capability across awake and various sleep states. The observed patterns of neonatal QEEG alterations in relation to PMA are consistent with the maturation of neonatal sleep, offering insights into the prediction and evaluation of brain development outcomes.

Keywords: quantitative EEG, neonates, sleep, postmenstrual age

Introduction

Sleep is fundamental to the growth, development, and restoration of the body, with its role being critically important in newborns and infants during the first year of life¹—a time characterized by rapid developmental changes.^{2,3} Sleep significantly contributes to brain maturation, enhancing learning and memory by optimizing synaptic architecture during periods of reduced neural network efficiency, thus facilitating energy conservation.^{4,5} REM sleep twitching is crucial not only for the development of sensory perception but also for motor skills.⁶ NREM sleep specifically enhances memories

tagged as relevant during waking periods, refining and optimizing memory networks.⁷ In mammals, sleep can improve learned motor skills⁸ and promote infants' recognition of stimuli.⁷

Additionally, sleep is not merely a simple negation of physiological sleep deprivation and disorders; it must also adapt to individual, social, and environmental needs to achieve physical and mental health.⁹ It is essential for emotional regulation, influencing the regulation of neurochemicals that affect emotional and stress responses.^{10,11} During early developmental stages, the quality of sleep is a critical determinant of future cognitive abilities and is associated with the emergence of psychopathological symptoms.^{12,13} Early sleep disturbances are linked with a range of negative outcomes, including compromised health, emotional dysregulation, impaired decision-making, reduced concentration, increased obesity risk, and diminished academic performance.¹⁴

The gold standard for monitoring neonatal sleep patterns is video electroencephalogram-polysomnography (EEG-PSG).^{15,16} EEG technology is widely utilized in the assessment of neonatal conditions and to monitor the efficacy of treatment such as hypoxic-ischemic encephalopathy and epileptic discharges, among other neurological disorders.^{17,18} However, interpreting raw EEG data for neonatal sleep staging is a resource-intensive task that demands substantial expertise and time, with skilled professionals required to analyze complex data over extended periods.

Quantitative Electroencephalography (QEEG) represents a progressive approach that builds on the traditional visual analysis of electroencephalographic data to extract specific metrics.¹⁹ This quantitative technique offers the potential to replace the intricate, laborious, and subjective process of manual EEG interpretation with a streamlined, rapid, and reproducible computer-assisted methodology, though it currently cannot completely detach from expert interpretation.²⁰ Unlike deep learning methods such as multi-branch convolutional neural networks,²¹ QEEG relies on hand-crafted feature-based classification, extracting various features from the time domain, frequency domain, and spatial domain.²² This allows for continuous, objective measurement of EEG activity and can be easily scaled to monitor a large number of newborns.²³

While QEEG has been widely applied in the evaluation of brain development in newborns with medical conditions,²⁴ research on the sleep of healthy newborns remains limited. Furthermore, there is a dearth of information on the evolution of QEEG parameters during the early postnatal period in correlation with postmenstrual age (PMA). This study utilizes 810 parameters composed of leads, spectral, and EEG features to examine full-term infants within the first week after birth to (1) delineate the range of QEEG parameters and identify those most effective in distinguishing between different sleep states; (2) explore the variations in QEEG parameters in relation to the progression of PMA.

Methods

Participants

This study recruited 60 neonates from September 2023 to February 2024 at a prominent obstetrics and gynecology hospital in China, which averages 8000 deliveries per year. The neonatal cohort presented various conditions, such as neonatal infections, hyperbilirubinemia, and wet lung. Inclusion criteria for the neonates were a gestational age between 37 and 42 weeks; no requirement for resuscitation post-delivery; and an Apgar score greater than 8 at 5 minutes post-birth. Exclusion criteria encompassed a maternal history of epilepsy^{25,26} or diabetes;²⁷ birth weight below 2.5 kg;²⁸ presence of congenital malformations or chromosomal abnormalities; inclusion in a multiple birth;²⁹ or technical issues with the EEG apparatus, like low power or electrode detachment. Since some infants do not require phototherapy, to ensure experimental consistency, we conducted EEG collections only when neonates were not undergoing phototherapy. All neonates in our cohort were in good general condition with no disease exacerbation during their hospital stay, and they were followed up in the outpatient clinic without any readmissions.

Recording Protocol

An attended polysomnogram lasting 3–6 hours was conducted after the infant was considered medically stable, necessitating no respiratory support and able to undergo a bedside polysomnogram. A polysomnographic technologist, present at the bedside, carefully documented behavioral observations throughout the session. The polysomnograms were later scored offline by the technologist and reviewed by an expert from the Children's Hospital of Fudan University, who

had specialized training and extensive experience in data annotation. The infants were housed in open bassinets, with routine care and feeding schedules (typically every three hours) maintained. Except during interventions like diaper changes, when recording was paused to reduce data interference, infants primarily stayed in the bassinets.

EEG Monitoring

EEG data were recorded using a Nicolet One machine (sampling frequency: 500 Hz), with electrode placement adhering to the neonate-modified 10–20 system endorsed by the American Clinical Neurophysiology Society.³⁰ Electrodes were positioned at the frontal pole (Fp1, Fp2), frontal (F3, F4), central (C3, C4), mid-temporal (T3, T4), and parietal (P3, P4) scalp regions, with a reference electrode at Cz. The parietal region (P3/P4) was chosen over the occipital (O1/O2) to minimize artifacts. The comprehensive setup included a 10-channel EEG, bilateral electrooculogram, chin electromyogram, oxygen saturation, electrocardiogram, and digital video recording.

EEG Sleep Staging Principles

Neonatal sleep staging was conducted in accordance with the AASM guidelines, utilizing EEG, EOG, and EMG data. The primary EEG derivations employed were F3-Cz, C3-Cz, and P3-Cz, with F4-Cz, C4-Cz, and P4-Cz serving as secondary options. Sleep stages were determined in 30-second intervals based on identifiable biomarkers within each epoch. The EEG trace, ancillary channel data, and video review were integral to identifying sleep states, in line with the American Clinical Neurophysiology Society's standard terminology and categorization for neonatal continuous EEG monitoring.³¹ For example, quiet sleep (QS) was classified into tracé alternant or slow-wave EEG patterns, whereas active sleep (AS) was identified by continuous, low-voltage waves. Additionally, the power spectrum of the EEG was crucial for differentiating between sleep stages, contributing to a more efficient analysis process.

EEG Pre-Processing and QEEG Features

The preprocessing steps employed the Auto-Neo-electroencephalography system from the Children's Hospital of Fudan University. Data were filtered (0.3 to 50 Hz), denoised, and subjected to Independent Component Analysis (ICA) to remove electrooculographic artifacts.

The QEEG features adhered to the characteristic indicators for neonates as outlined by John M. O'Toole and Geraldine B. Boylan.³² An exhaustive extraction of 810 neural signal features was performed, encompassing amplitude, rEEG, spectral density, and connectivity. Initially, the signal data were segmented into four frequency bands: delta (0.5–4 Hz), theta (4–8 Hz), alpha (8–13 Hz), and beta (13–30 Hz), across ten channels. For each band and channel, a set of features were calculated: six related to amplitude (total power, standard deviation, skewness, kurtosis, envelope mean, envelope standard deviation), eight to rEEG (mean, median, lower margin, upper margin, width, standard deviation, coefficient of variation, asymmetry), and five to spectral aspects (absolute power, relative power, flatness (Wiener entropy), entropy (Shannon entropy), difference), resulting in 760 features $[(6+8+5) * 4 \text{ (frequency bands)} * 10 \text{ (channels)}]$. Additionally, three spectral features (95th and 50th percentile spectral edge frequencies, fractal dimension) across ten channels yielded 30 features $(3 * 10 \text{ channels})$. Moreover, five connectivity features (brain symmetry index, correlation (Pearson), mean coherence, maximum coherence, frequency of maximum coherence) per frequency band resulted in 20 features. In total, this approach enabled the extraction of 810 $(760+30+20)$ neural signal features per sample, illustrating a comprehensive methodology for the quantitative analysis of neural signals.

Statistical Analysis

Descriptive statistical measures, namely mean and standard deviation (SD), were employed to summarize the normative data of QEEG across different states of consciousness, including awake, AS, and QS. The assessment of data normality was conducted using histogram analysis and the Shapiro–Wilk test. To determine the differences in QEEG parameters across various sleep states, a comprehensive analysis utilizing repeated measures of variance (the Friedman test) was performed. If the global analysis indicated significant results, post-hoc pairwise comparisons were conducted using the Wilcoxon signed-rank test. To adjust for the heightened risk of Type I error arising from multiple pairwise comparisons across the three sleep states, a Bonferroni correction was applied to the p-values from these posthoc tests. A p-value of

less than 0.05 was considered statistically significant. Additionally, the discriminative ability of QEEG parameters to differentiate between the sleep states was assessed using receiver operating characteristic (ROC) curves. The 95% confidence interval for the area under the curve (AUC) was determined using DeLong's method. The optimal cutoff points for each QEEG parameter were identified by maximizing the Youden index (sensitivity + specificity - 1).

The influence of postmenstrual age (PMA) on QEEG features was examined through multivariable linear regression analysis using the Stepwise Method. This method allowed for the calculation of β weights (standardized regression coefficients), which indicate the extent of change, in standard deviation units, in the dependent variable for each standard deviation increase in the independent variable. To reduce the risk of Type I error associated with multiple comparisons, a more stringent significance threshold of 0.01 was set for all multivariable linear regression analyses.

Results

Demographics

Table 1 presents demographic details for the 54 full-term neonates included in the study, comprising 26 males and 28 females. Among the 54 infants, 15 were delivered by cesarean section. Of these, 36 infants (66.67%) were admitted due to hyperbilirubinemia, 20 infants (37.04%) due to infections, and 1 infant (1.85%) due to wet lung. These neonates underwent EEG examinations within the first 7 days post-birth, contingent on their physical condition. The mean gestational age (standard deviation) was 39.50 (1.14) weeks, the mean post-menstrual age was 40.11 (1.12) weeks, the age post-birth was 4.31 (1.68) days, and the birth weight was 3309.06 (328.65) grams. On average, each newborn was recorded for 248.08 (46.37) minutes.

We also compared whether cesarean delivery, hyperbilirubinemia, and infections influence EEG indices. Since only one newborn was diagnosed with wet lung, we did not analyze this potential influencing factor. The only significant finding was in the theta frequency band's spectral flatness (AS_4_8_spectral_flatness_Fp1) in lead F1, which differed between the cesarean and vaginal delivery groups, with a P-value of 0.0133. However, given that we analyzed a total of 810 indices and found only one positive result, this finding is not convincing.

QEEG Differentiation of Various Sleep Stages

With numerous computational indices at our disposal, we highlighted the top 20 indices based on the AUC from the ROC analysis, capable of differentiating between various sleep stages.

Figures 1A, 2A, and 3A rank the top 20 QEEG parameters by their efficacy in distinguishing between awake and sleep states, as determined by the ROC analysis AUC. Predominantly, spectral differences within the alpha and beta frequency bands were the most effective in differentiating between AS and QS, as depicted in **Figure 1A**. The alpha band spectral difference at the F3 lead emerged as the most discriminating parameter with an AUC of 0.88, closely followed by the beta band spectral difference at the C4 lead with an AUC of 0.87. In distinguishing between Awake and AS stages (**Figure 2A**), the

Table 1 Demographics

N = 54	Mean \pm std	Range
Sex, Female/male	28/26	–
Mode of delivery, CS/VD	15/39	
Record time (mins)	248.08 \pm 46.37	188~361
Gestational age (weeks)	39.50 \pm 1.14	37.14~41.29
Postmenstrual age (weeks)	40.11 \pm 1.12	37.71~41.86
Chronological age (days)	4.31 \pm 1.68	1~7
Birth weight (grams)	3309.06 \pm 328.65	2640~4200
Reasons for admission		
Hyperbilirubinemia	36 (66.67%)	
Infections	20 (37.04%)	
Wet lung	1 (1.85%)	

Abbreviations: CS, cesarean section; VD, vaginal delivery.

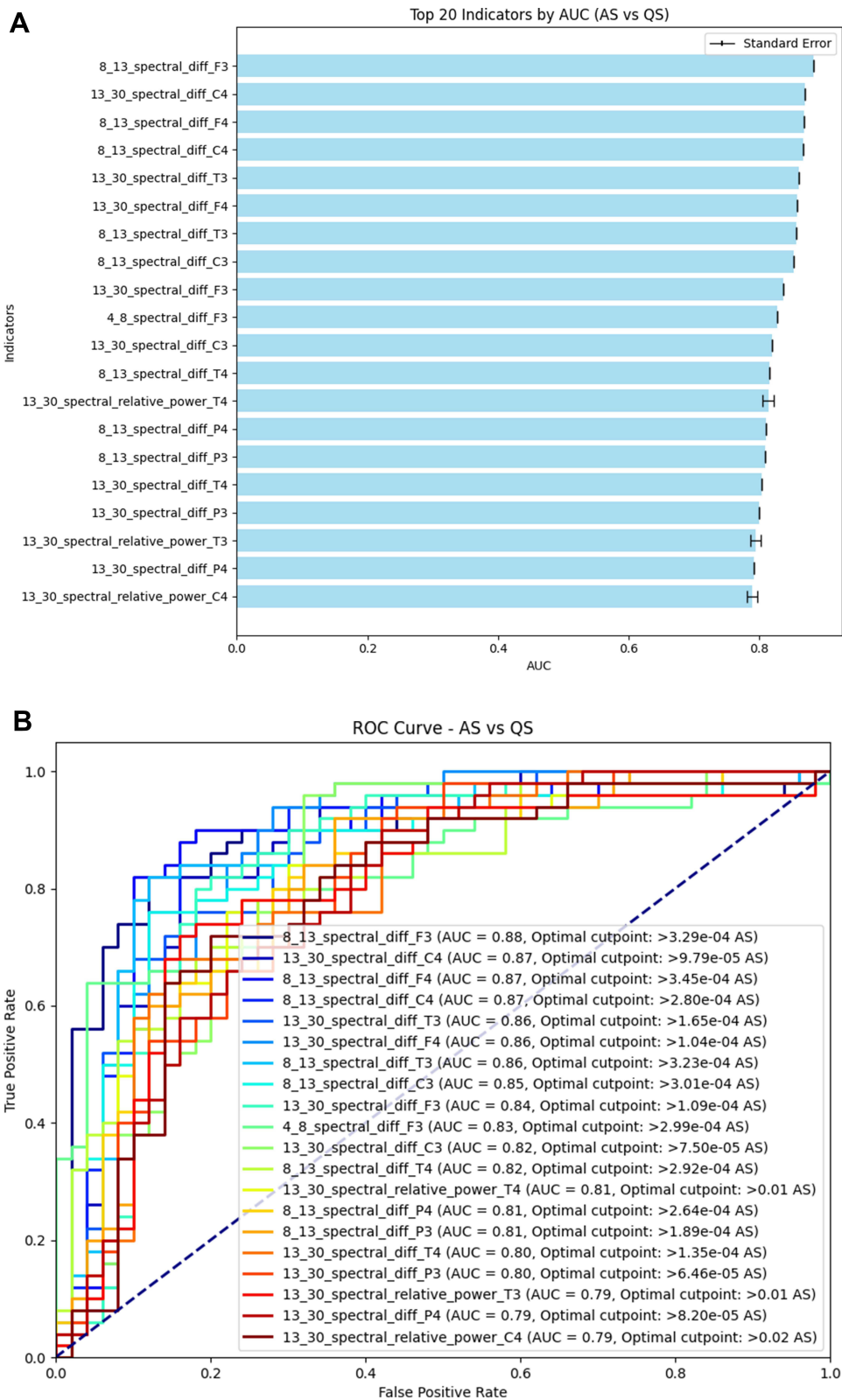


Figure 1 The ROCAUC of the top 20 parameters that differentiate between AS and QS. **(A)** shows the top 20 indicators that distinguish between AS and QS periods and their corresponding ROC-AUC values. The blue bars represent the ranking of ROC-AUC values, and the T-shaped black lines indicate the standard error. **(B)** displays the ROC curves, with the legend showing the color lines corresponding to the 20 indicators. The values and specific details of these indicators can be found in [Supplementary Table 1](#).

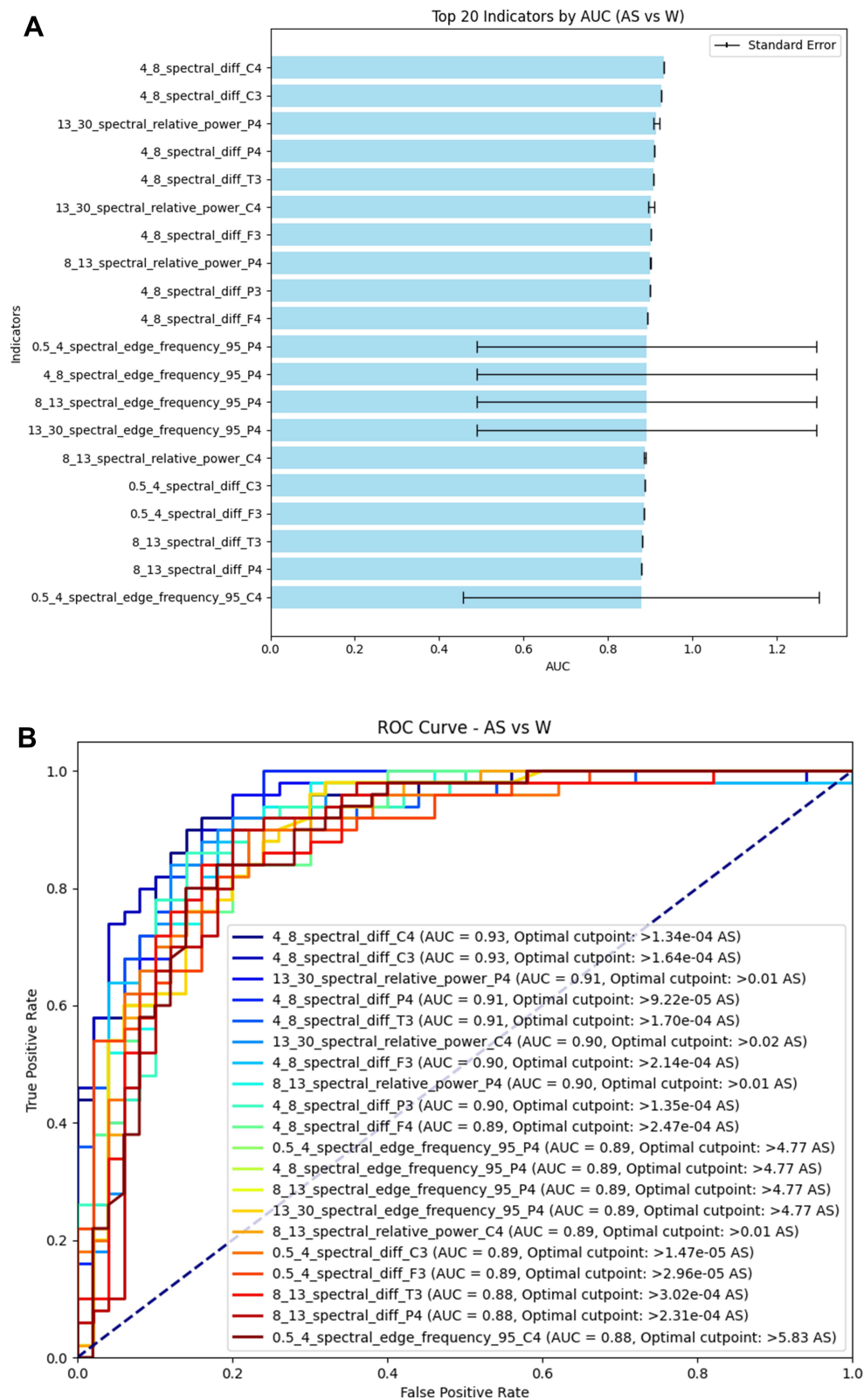


Figure 2 The ROCAUC of the top 20 parameters that differentiate between AS and W. **(A)** shows the top 20 indicators that distinguish between AS and W periods and their corresponding ROC-AUC values. The blue bars represent the ranking of ROC-AUC values, and the T-shaped black lines indicate the standard error. **(B)** displays the ROC curves, with the legend showing the color lines corresponding to the 20 indicators. The values and specific details of these indicators can be found in [Supplementary Table 2](#).

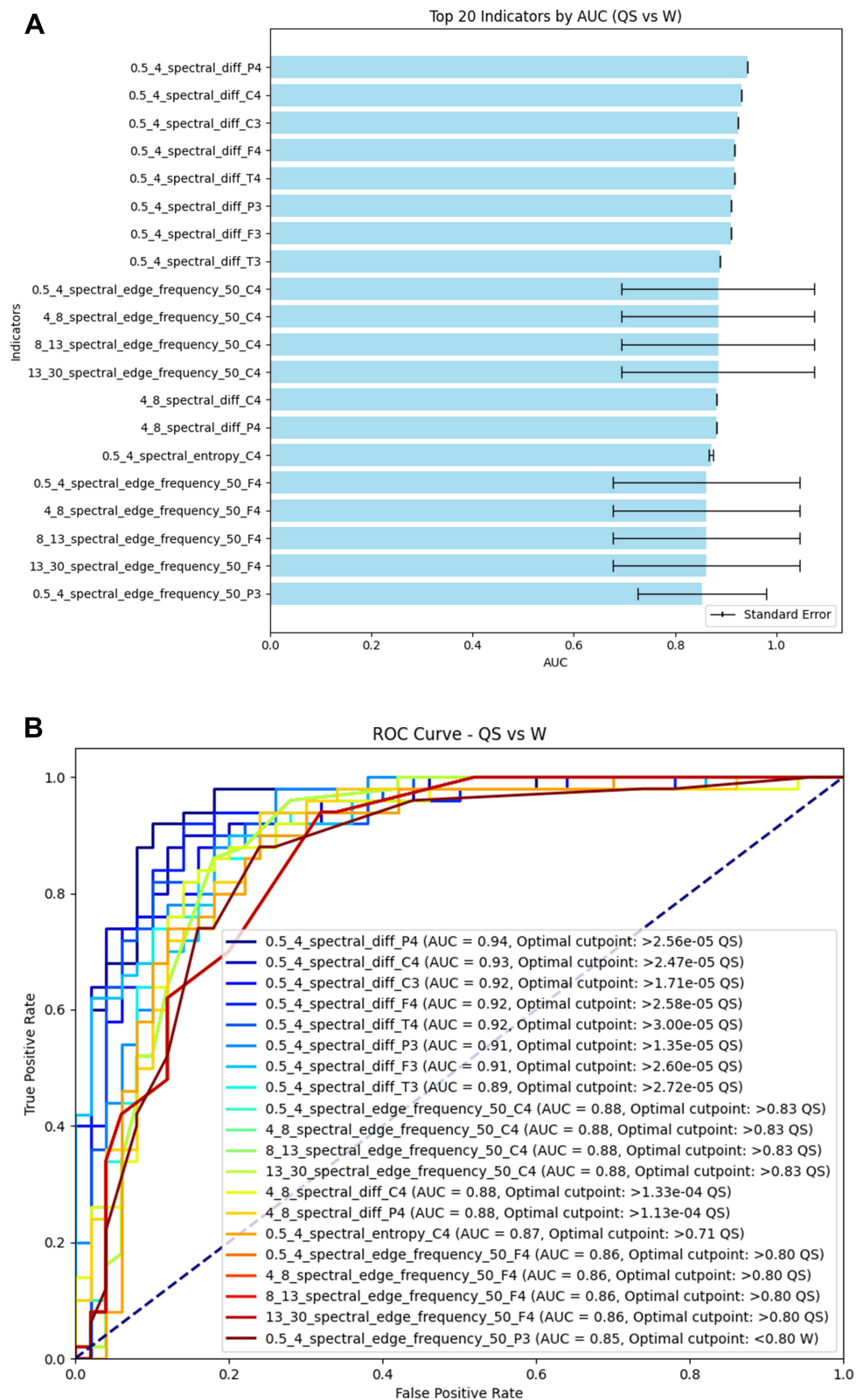


Figure 3 The ROCAUC of the top 20 parameters that differentiate between QS and W. **(A)** shows the top 20 indicators that distinguish between QS and W periods and their corresponding ROC-AUC values. The blue bars represent the ranking of ROC-AUC values, and the T-shaped black lines indicate the standard error. **(B)** displays the ROC curves, with the legend showing the color lines corresponding to the 20 indicators. The values and specific details of these indicators can be found in [Supplementary Table 3](#).

theta band spectral difference and relative power showed significant differentiation capability, with the theta spectral difference at the C4 and C3 leads achieving an AUC of 0.93, and the beta band spectral relative power at the P4 lead reaching an AUC of 0.91. Theta band spectral differences at the F3, F4, P3, P4, and T3 leads, alongside theta band spectral relative power at the C4 and alpha band spectral relative power at the P4 leads, all surpassed an AUC of 0.90. Regarding the differentiation between QS and Wakefulness (Figure 3A), the delta band spectral differences and the 50% spectral edge frequency across various bands showed strong discriminative capacities, with the delta band spectral difference at the P4 lead attaining the highest AUC of 0.94, and the 50% spectral edge frequencies at the C4 across all bands each exhibiting an AUC of 0.88.

Figures 1B, 2B, and 3B display the ROC curves for QEEG parameters that effectively differentiate between awake and sleep states. Tables 2–4 detail the AUC values for the top 5 parameters along with their 95% confidence intervals. Detailed information on the top 20 parameters by AUC can be found in [Supplementary Tables 1–3](#)

QEEG Changes with Postmenstrual Age

[Supplementary Figures 1–3](#) illustrate the trends in QEEG changes relative to PMA. [Tables 5–7](#) present the regression model coefficients and P-values for the wakefulness, AS, and QS phases, respectively. When encountering multiple leads all correlating

Table 2 The Top 5 Parameters Capable of Distinguishing Between as and QS

Indicator	AUC	AUC 95% CI	Best Cutoff
8_13_spectral_diff_F3	0.88	(4.74e-5, 6.68e-4)	3.29e-4
13_30_spectral_diff_C4	0.87	(1.50e-5, 4.43e-4)	9.79e-5
8_13_spectral_diff_F4	0.87	(1.07e-4, 6.84e-4)	3.45e-4
8_13_spectral_diff_C4	0.87	(5.22e-5, 6.81e-4)	2.80e-4
13_30_spectral_diff_T3	0.86	(3.02e-5, 4.05e-4)	1.65e-4

Abbreviations: AUC, area under the receiver operator characteristics curve; CI, confidence interval; Cutoff values associated with minimal false-negative and positive results are shown. Data are expressed with a 95% CI.

Table 3 The Top 5 Parameters Capable of Distinguishing Between as and W

Indicator	AUC	AUC 95% CI	Best Cutoff
4_8_spectral_diff_C4	0.93	(6.43e-6, 4.02e-4)	1.34e-4
4_8_spectral_diff_C3	0.93	(5.28e-6, 4.18e-4)	1.64e-4
13_30_spectral_relative_power_P4	0.91	(2.62e-3, 6.44e-2)	1.42e-2
4_8_spectral_diff_P4	0.91	(3.19e-6, 4.32e-4)	9.22e-5
4_8_spectral_diff_T3	0.91	(6.99e-6, 4.16e-4)	1.70e-4

Abbreviations: AUC, area under the receiver operator characteristics curve; CI, confidence interval; Cutoff values associated with minimal false-negative and positive results are shown. Data are expressed with a 95% CI.

Table 4 The Top 5 Parameters Capable of Distinguishing Between QS and W

Indicator	AUC	AUC 95% CI	Best Cutoff
0.5_4_spectral_diff_P4	0.94	(1.23e-6, 1.55e-4)	2.56e-5
0.5_4_spectral_diff_C4	0.93	(1.49e-6, 1.50e-4)	2.47e-5
0.5_4_spectral_diff_C3	0.92	(1.09e-6, 1.51e-4)	1.71e-5
0.5_4_spectral_diff_F4	0.92	(1.59e-6, 2.06e-4)	2.58e-5
0.5_4_spectral_diff_T4	0.92	(1.41e-6, 1.25e-4)	3.00e-5

Abbreviations: AUC, area under the receiver operator characteristics curve; CI, confidence interval; Cutoff values associated with minimal false-negative and positive results are shown. Data are expressed with a 95% CI.

Table 5 The Pattern of Changes in QEEG Parameters During the Wakeful State Across Postmenstrual Age

Spectral Power	Signal Features	R ²	Beta	P value
13_30	Spectral_entropy_F3	0.14	0.0004	<0.01
	Spectral_entropy_F4	0.14	0.0004	<0.01
	Spectral_flatness_F3	0.14	0.0012	<0.01

Table 6 The Variation Pattern of QEEG Parameters During as Across Postmenstrual Age

Spectral Power	Signal Features	R ²	Beta	P value
0.5_4	Spectral_edge_frequency_95_C3	0.15	0.2014	<0.01
	Spectral_entropy_C4	0.28	0.0019	<0.01
	Spectral_entropy_F4	0.31	0.0024	<0.01
	Spectral_entropy_P3	0.21	0.002	<0.01
	Spectral_flatness_F3	0.32	0.0037	<0.01
	Spectral_flatness_F4	0.35	0.0039	<0.01
4_8	Spectral_edge_frequency_95_C3	0.15	0.2014	<0.01
	Spectral_relative_power_C3	0.34	0.0012	<0.01
	Spectral_relative_power_F4	0.32	0.0012	<0.01
8_13	rEEG_asymmetry_P3	0.15	-0.0035	<0.01
	Spectral_edge_frequency_95_C3	0.13	0.2014	<0.01
	Spectral_entropy_P4	0.13	-0.0001	<0.01
	Spectral_flatness_C4	0.18	-0.0005	<0.01
	Spectral_relative_power_C3	0.13	0.0006	<0.01
	Spectral_relative_power_F4	0.14	0.0005	<0.01
13_30	rEEG_CV_P3	0.14	-0.0046	<0.01
	Spectral_edge_frequency_95_C3	0.15	0.2014	<0.01

Table 7 The Variation Pattern of QEEG Parameters During QS Across Postmenstrual Age

Spectral Power	Signal Features	R ²	Beta	P value
4_8	Spectral_entropy_F3	0.53	0.0029	<0.01
	Spectral_entropy_F4	0.53	0.0033	<0.01
	Spectral_flatness_F3	0.55	0.0048	<0.01
	Spectral_flatness_F4	0.55	0.0054	<0.01
	Spectral_diff_P3	0.16	4.54E-06	<0.01
	Spectral_relative_power_C3	0.413	0.0014	<0.01
	Spectral_relative_power_P3	0.5	0.0013	<0.01
	Spectral_entropy_F3	0.17	-0.0002	<0.01
	Spectral_entropy_P4	0.33	-0.0002	<0.01
	Spectral_flatness_F3	0.19	-0.0007	<0.01
	Spectral_relative_power_C3	0.14	0.0004	<0.01
13_30	Spectral_relative_power_P3	0.16	0.0003	<0.01
	rEEG_asymmetry_C3	0.23	-0.0074	<0.01
	rEEG_asymmetry_P3	0.22	-0.0076	<0.01
	rEEG_CV_F4	0.17	-0.0064	<0.01
	Spectral_diff_C3	0.16	4.33E-06	<0.01
	Spectral_diff_T3	0.17	4.34E-06	<0.01

with post-menstrual age for the same indicator, we have retained only the two leads with the best fit (ie, the highest R^2) in Table 6 and Table 7. The complete data for these indicators can be found in [Supplementary Tables 4 and 5](#). During wakefulness ([Supplementary Figure 1A–C](#) and Table 5), there was an observed increase in both Wiener and Shannon entropy within the beta frequency band of the frontal lobe correlating with PMA. In the AS phase ([Supplementary Figure 2](#) and Table 6) and the QS phase ([Supplementary Figure 3](#) and Table 7), an increase in entropy within the delta frequency band across all monitored brain regions was noted (AS: [Supplementary Figure 2B–Q](#)) (QS: [Supplementary Figure 3A–P](#)). Additionally, the spectral relative power within the theta frequency band also showed an upward trend with PMA during both AS ([Supplementary Figure 2S–Z](#)) and QS ([Supplementary Figure 3R–Y](#)) phases.

Specifically, during the AS phase, there was a decrease in rEEG asymmetry within the alpha frequency band at the P3 lead ([Supplementary Figure 2AA](#)), and in the beta frequency band across the temporal and parietal lobes during the QS phase ([Supplementary Figure 3AG–AJ](#)) associated with increasing PMA. Moreover, the 95% spectral edge frequency in every frequency band within the midline central area exhibited an upward trend with PMA during the AS phase ([Supplementary Figure 2A, R, AB and AH](#)).

In the QS phase, an increase in spectral relative power within the alpha frequency band across the frontal, central, and parietal lobes was observed with advancing PMA ([Supplementary Figure 3AD–AF](#)), while entropy showed a decrease ([Supplementary Figure 3Z–AC](#)). Additionally, there was an increase in spectral difference within the beta frequency band across the frontal, central, and parietal lobes correlated with PMA ([Supplementary Figure 3AL–AR](#)).

Discussion

The index that was most capable of distinguishing between AS and QS stages was the spectral difference within the alpha frequency band at the F3 electrode (spectral_diff_F3). The theta frequency spectral difference at the C4 electrode (spectral_diff_C4) proved to be the most effective in differentiating AS from wakefulness (W), while the delta frequency spectral difference at the P4 electrode (spectral_diff_P4) was the best at distinguishing QS from W. During the AS and QS phases, there was an observed increase in entropy within the delta frequency band across all monitored brain regions and an increase in the spectral relative power within the theta frequency band with PMA. Additionally, there was a decrease in rEEG asymmetry within the alpha frequency band at the P3 lead during the AS phase, and a decrease in the beta frequency band rEEG asymmetry across the temporal and parietal lobes during the QS phase, associated with increasing PMA.

The association of QEEG parameters with outcomes in neonatal sleep research, particularly concerning growth and development, was notable. A greater proportion of quiet sleep and higher state entropy were correlated with poorer neurological examination scores, whereas decreased delta power during quiet sleep was associated with better examination outcomes ($\rho = -0.43$, $p = 0.023$).³³

Innovative EEG Metrics for Differentiating Sleep Stages

This study employed hundreds of EEG indices to differentiate between sleep stages, identifying the most discriminative markers. The primary indices for distinguishing between sleep and wakefulness phases were mainly spectral difference measures, an aspect not extensively explored in previous research. Other indices like spectral entropy and Spectral Edge Frequency (SEF) had been validated in earlier studies for their ability to differentiate sleep stages.^{34,35}

Spectral difference, defined as the change in spectra between consecutive time segments in a spectrogram³² – a visual representation of the frequency spectrum of a signal over time obtained through Short-Time Fourier Transform (STFT) – was significantly discriminative. The superior discriminative power of spectral difference in distinguishing between various sleep stages may be attributed to the distinct predominant frequency bands characteristic of neonatal wakefulness and sleep phases.³⁶ For example, wakefulness was typically marked by theta activity with low-voltage, irregular delta waves, AS by mixed-wave activity, and QS predominantly by delta slow waves, with occasional theta waves. This variation in primary frequency bands across sleep states highlighted the effectiveness of spectral difference as a discriminating feature.

We introduced the parameter of spectral flatness, also known as Wiener entropy, along with Shannon entropy (spectral entropy), to quantify the uniformity of the spectral distribution.³⁷ These metrics showed trends that consistently aligned

Table 8 Comparison of Different Research for QEEG in Neonatal Sleep Stages

Study	Year	Authors	Demographics	EEG channel	Features	Sleep stage	Results
Comparison of quantitative EEG characteristics of quiet and active sleep in newborns ⁴³	2003	Karel Paul, Vladimír Krajca, et al	21 healthy newborns (10 full-term and 11 pre-term)	Fp1, Fp2, C3, C4, O1, O2, T3, T4	AV, Mm, $\delta 1$, $\delta 2$, $\theta 1$, $\theta 2$, α , D1 and D2; L and MF; No and t%*	Two sleep classes (AS and QS)	AS vs QS: (a) the number and length of quasi-stationary segments, (b) voltage and (c) power in delta and theta bands
EEG in the healthy term newborn within 12 hours of birth ³⁴	2012	I Korotchkova, S Connolly, et al	30 normal newborn babies	F4, F3, Cz, T4, T3, P4, P3	SEF, H, and δ_R	Two sleep classes (AS and QS)	SEF and H were significantly higher ($p < 0.0001$) and δ_R was significantly lower ($p < 0.0001$) in AS than in QS.
Quantitative electroencephalogram in term neonates under different sleep states ³⁵	2023	Ian Yuan, Georgia Georgostathi, et al	30 normal neonates 37 to 46 weeks suspected seizure or differential diagnosis of apneic episodes	Fp1-C3, Fp2-C4	Total power, power ratio, coherence, entropy, and SEF 50 and 90	Three sleep classes (AS, QS and Wake)	Awake vs AS: Entropy beta AUC-ROC > 0.84; Awake vs QS: Entropy beta, entropy delta I, theta power %, and SEF50 AUC-ROC > 0.78 AS vs QS: theta power % AUC-ROC > 0.69

Notes: *The features used in paper: AV—standard deviation of the sample values in the segment; Mm—the difference between maximal positive and minimal negative values of the samples in the segment; D1—maximum of absolute values of the first derivative of the samples in the segment; D2—maximum of absolute values of the second derivative of the samples in the segment; MF—average frequency of the EEG activity in the segment; t%—time percentage of the relevant class occurrence; No—number of segments of the relevant class; L—average duration of the relevant class segments.

Abbreviations: AS, active sleep; QS, quiet sleep; SEF, spectral edge frequency; H, spectral entropy; δ_R : relative delta power.

with changes in corrected gestational age. Notably, during the quiet and active sleep phases, the entropy within the Delta frequency band increased with corrected gestational age, indicating a rise in complexity within this band,³⁸ which includes a broader spectrum of waveforms. This increase may signify the gradual transition from neonatal sleep patterns to those typical of childhood, characterized by the emergence of slow-wave sleep (0.5Hz-2Hz).³⁹

rEEG has been shown to vary with corrected gestational age in preterm infants and is associated with growth and developmental outcomes.⁴⁰ In term neonates, we observed that rEEG asymmetry in the beta frequency band decreased with increasing corrected gestational age. Voltage asymmetry in a single channel, attributed to positional shifts over time, originates from a limited number of neurons firing synchronously at the same frequency during infancy.⁴⁰ However, as age progresses, the number of synchronously firing neurons increases, leading to a gradual synchronization of brain discharges. Consistent with previous findings,⁴¹ our results also confirmed that during both AS and QS phases, theta waves increased with corrected gestational age, serving as an indicator of brain maturation. Particularly noteworthy was the gradual increase in the relative spectral power of the Alpha frequency band during the QS phase with advancing corrected gestational age, potentially associated with the progressive emergence of sleep spindles (10Hz-16Hz).⁴² This observation underscores the developmental progression in neural activity patterns, indicative of advancing neurological maturity and the evolving complexity of sleep architecture in the developing brain.

Innovations and Advantages of This Study

Our study results have established the EEG characteristics of low-risk term infants admitted to the neonatal unit within the first week after birth. In [Table 8](#), we have listed the contributions made by previous researchers on neonatal sleep QEEG. Previous researchers have long used QEEG to explore differences in various sleep stages,⁴³ but they only identified differences without using ROC analysis to determine which metrics contributed the most. Additionally, they primarily focused on AS and QS stages, neglecting the awake period.^{34,43} Considering that newborns exhibit significant movement during sleep, including the awake period in the study provides a more comprehensive and rigorous analysis. Recent studies have used some metrics from Amplitude, Spectral, and Connectivity features to explore which indicators can better distinguish between the three stages.³⁵ Unlike previous studies with smaller sample sizes,^{34,35} our inclusion of 54 normal neonates enabled us to provide more robust evidence. By extracting a comprehensive set of features, we identified more effective metrics for distinguishing different sleep stages.

Specifically, the alpha band spectral difference at the F3 lead was the most discriminating parameter between AS and QS, with an AUC of 0.88. The theta spectral difference at the C4 and C3 leads showed significant differentiation capability between Awake and AS stages, achieving an AUC of 0.93. The delta band spectral difference at the P4 lead demonstrated strong discriminative capacity between QS and Wakefulness, attaining the highest AUC of 0.94. Finally, we have provided, for the first time, a distribution of healthy neonatal brain EEG characteristics and explored the relationship between quantitative EEG features and postnatal age. This extensive collection of features has allowed us to develop machine learning-based models for individual-level predictions, laying the foundation for precision medicine.

Limitations and Future Research Directions

The limitations of our study include its design as a single-center experiment. While we collected a relatively large sample size compared to prior studies,^{34,35,43} validation through multi-center studies would be advantageous for future research, enhancing the generalizability and robustness of the findings. This expanded approach could offer a more comprehensive understanding of the research topic. Additionally, due to the presence of numerous artifacts in the occipital lobe, we were unable to monitor the occipital brain regions. Future research may need to employ innovative equipment to ensure comprehensive monitoring of each brain area.

Conclusion

In summary, our study identified more effective QEEG metrics for distinguishing between awake and sleep states, as well as delineated the developmental characteristics of cortical activity across different sleep-wake states in a normal neonatal cohort. Notably, the spectral difference emerged as the parameter with the highest overall discriminative capacity for differentiating between awake and various sleep states. The observed patterns of neonatal QEEG changes in relation to

PMA align with the developmental trajectory of neonatal sleep. The application of QEEG analysis provides valuable objective data that can enhance traditional methods of neonatal sleep staging, thereby facilitating the development of more comprehensive machine-learning models aimed at predicting neurodevelopmental outcomes. This integration of QEEG with machine learning approaches holds the potential to advance our understanding and monitoring of neonatal brain development significantly.

Data Sharing Statement

The datasets used and/or analyzed during the current study are available from the corresponding author upon reasonable request.

Ethics Approval and Consent to Participate

The research ethics committee of the Obstetrics and Gynecology Hospital of Fudan University approved this study (approval No. (2023) 99), and informed written consent was obtained from the parents before participation. The study adhered to the ethical standards delineated in the Declaration of Helsinki guidelines.

Consent for Publication

All authors consent to publication.

Acknowledgments

We would like to acknowledge Shanghai Songjiang Center For Primate Brain Research and the Shanghai Quanlan Technology development team for their hard work on the LANMAO Sleep Recorder both in hardware and software.

Author Contributions

All authors made a significant contribution to the work reported, whether that is in the conception, study design, execution, acquisition of data, analysis and interpretation, or in all these areas; took part in drafting, revising or critically reviewing the article; gave final approval of the version to be published; have agreed on the journal to which the article has been submitted; and agree to be accountable for all aspects of the work.

Funding

2023 Young Clinical Full-time Research Team of Shanghai Medical College, Fudan University Funder: Shanghai Medical College Fudan University Recipient: Xinran Dong. Science and Technology Innovation Program of Shanghai (20Z11900603 to Jimei Wang).

Disclosure

The authors declare no competing interests.

References

1. Graven SN, Browne JV. Sleep and brain development: the critical role of sleep in fetal and early neonatal brain development. *Newborn Infant Nurs Rev.* 2008;8(4):173–179. doi:10.1053/j.nainr.2008.10.008
2. Hong H, Maloney MA, Keens TG, Perez IA. Sleep in Infants. *Am J Respir Crit Care Med.* 2018;198(8):P15–p6. doi:10.1164/rccm.1988P15
3. Pierce LJ, Thompson BL, Gharib A, et al. Association of perceived maternal stress during the perinatal period with electroencephalography patterns in 2-month-old infants. *JAMA Pediatr.* 2019;173(6):561–570. doi:10.1001/jamapediatrics.2019.0492
4. Li W, Ma L, Yang G, Gan WB. REM sleep selectively prunes and maintains new synapses in development and learning. *Nat Neurosci.* 2017;20(3):427–437. doi:10.1038/nn.4479
5. Tononi G, Cirelli C. Sleep and the price of plasticity: from synaptic and cellular homeostasis to memory consolidation and integration. *Neuron.* 2014;81(1):12–34. doi:10.1016/j.neuron.2013.12.025
6. Blumberg MS, Coleman CM, Gerth AI, McMurray B. Spatiotemporal structure of REM sleep twitching reveals developmental origins of motor synergies. *Curr Biol.* 2013;23(21):2100–2109. doi:10.1016/j.cub.2013.08.055
7. Stickgold R, Walker MP. Sleep-dependent memory triage: evolving generalization through selective processing. *Nat Neurosci.* 2013;16(2):139–145. doi:10.1038/nn.3303

8. Vyazovskiy VV, Harris KD. Sleep and the single neuron: the role of global slow oscillations in individual cell rest. *Nat Rev Neurosci.* 2013;14(6):443–451. doi:10.1038/nrn3494
9. Buysse DJ. Sleep health: can we define it? Does it matter? *Sleep.* 2014;37(1):9–17. doi:10.5665/sleep.3298
10. Mindell JA, Lee C. Sleep, mood, and development in infants. *Infant Behav Dev.* 2015;41:102–107. doi:10.1016/j.infbeh.2015.08.004
11. Brinkman JE, Reddy V, Sharma S. Physiology of Sleep. In: *StatPearls*. Treasure Island (FL): StatPearls Publishing LLC; 2024.
12. Sadeh A, Tikotzky L, Kahn M. Sleep in infancy and childhood: implications for emotional and behavioral difficulties in adolescence and beyond. *Curr Opin Psychiatry.* 2014;27(6):453–459.
13. Bertrand SJ, Zhang Z, Patel R, et al. Transient neonatal sleep fragmentation results in long-term neuroinflammation and cognitive impairment in a rabbit model. *Exp Neurol.* 2020;327:113212. doi:10.1016/j.expneurol.2020.113212
14. Chaput JP, Gray CE, Poitras VJ, et al. Systematic review of the relationships between sleep duration and health indicators in school-aged children and youth. *Appl Physiol Nutr Metab.* 2016;41(6 Suppl 3):S266–82. doi:10.1139/apnm-2015-0627
15. Dos Santos AA, Khan RL, Rocha G, Nunes ML. Behavior and EEG concordance of active and quiet sleep in preterm very low birth weight and full-term neonates at matched conceptual age. *Early Human Dev.* 2014;90(9):507–510. doi:10.1016/j.earlhumdev.2014.06.014
16. Barbeau DY, Weiss MD. Sleep Disturbances in Newborns. *Children.* 2017;4(10). doi:10.3390/children4100090
17. Nash KB, Bonifacio SL, Glass HC, et al. Video-EEG monitoring in newborns with hypoxic-ischemic encephalopathy treated with hypothermia. *Neurology.* 2011;76(6):556–562. doi:10.1212/WNL.0b013e31820af91a
18. Hoque N, Chakkarapani E, Liu X, Thoresen M. A comparison of cooling methods used in therapeutic hypothermia for perinatal asphyxia. *Pediatrics.* 2010;126(1):e124–30. doi:10.1542/peds.2009-2995
19. O’Toole JM, Boylan GB. Quantitative Preterm EEG analysis: the need for caution in using modern data science techniques. *Front Pediatr.* 2019;7:174. doi:10.3389/fped.2019.00174
20. Ryan MAJ, Malhotra A. Electrographic monitoring for seizure detection in the neonatal unit: current status and future direction. *Pediatr Res.* 2024. doi:10.1038/s41390-024-03207-2
21. Siddiq HA, Tang ZN, Xu Y, et al. Single-Channel EEG data analysis using a multi-branch CNN for neonatal sleep staging. *IEEE Access.* 2024;12:29910–29925. doi:10.1109/ACCESS.2024.3365570
22. Abbasi SF, Abbas A, Ahmad I, et al. Automatic neonatal sleep stage classification: a comparative study. *Heliyon.* 2023;9(11):e22195. doi:10.1016/j.heliyon.2023.e22195
23. O’Toole JM, Mathieson SR, Raurale SA, et al. Neonatal EEG graded for severity of background abnormalities in hypoxic-ischaemic encephalopathy. *Sci Data.* 2023;10(1):129. doi:10.1038/s41597-023-02002-8
24. Wang X, Trabatti C, Weeke L, et al. Early qualitative and quantitative amplitude-integrated electroencephalogram and raw electroencephalogram for predicting long-term neurodevelopmental outcomes in extremely preterm infants in the Netherlands: a 10-year cohort study. *Lancet Digit Health.* 2023;5(12):e895–e904. doi:10.1016/S2589-7500(23)00198-X
25. Shellhaas RA, Wusthoff CJ, Tsuchida TN, et al. Profile of neonatal epilepsies: characteristics of a prospective US cohort. *Neurology.* 2017;89(9):893–899. doi:10.1212/WNL.0000000000004284
26. Videman M, Tokariev A, Stjerna S, Roivainen R, Gaily E, Vanhatalo S. Effects of prenatal antiepileptic drug exposure on newborn brain activity. *Epilepsia.* 2016;57(2):252–262. doi:10.1111/epi.13281
27. Castro Conde JR, González González NL, González Barrios D, González Campo C, Suárez Hernández Y, Sosa Comino E. Video-EEG recordings in full-term neonates of diabetic mothers: observational study. *Arch Dis Child Fetal Neonatal Ed.* 2013;98(6):F493–8. doi:10.1136/archdischild-2013-304283
28. Stevenson NJ, Lai MM, Starkman HE, Colditz PB, Wixey JA. Electroencephalographic studies in growth-restricted and small-for-gestational-age neonates. *Pediatr Res.* 2022;92(6):1527–1534. doi:10.1038/s41390-022-01992-2
29. Vucinovic M, Kardum G, Bonkovic M, Resic B, Ursic A, Vukovic J. Sleep EEG composition in the first three months of life in monozygotic and dizygotic twins. *Clin Eeg Neurosci.* 2014;45(3):193–200. doi:10.1177/1550059413497000
30. Shellhaas RA, Chang T, Tsuchida T, et al. The American clinical neurophysiology society’s guideline on continuous electroencephalography monitoring in neonates. *J Clin Neurophysiol.* 2011;28(6):611–617. doi:10.1097/WNP.0b013e31823e96d7
31. Tsuchida TN, Wusthoff CJ, Shellhaas RA, et al. American clinical neurophysiology society standardized EEG terminology and categorization for the description of continuous EEG monitoring in neonates: report of the American clinical neurophysiology society critical care monitoring committee. *J Clin Neurophysiol.* 2013;30(2):161–173. doi:10.1097/WNP.0b013e3182872b24
32. O’Toole J, Boylan G. NEURAL: quantitative features for newborn EEG using Matlab. *arXiv e-prints.* 2017;2017:1.
33. Shellhaas RA, Burns JW, Barks JD, Chervin RD. Quantitative sleep stage analyses as a window to neonatal neurologic function. *Neurology.* 2014;82(5):390–395. doi:10.1212/WNL.0000000000000085
34. Korotchkova I, Connolly S, Ryan CA, et al. EEG in the healthy term newborn within 12 hours of birth. *Clin Neurophysiol.* 2009;120(6):1046–1053. doi:10.1016/j.clinph.2009.03.015
35. Yuan I, Georgostathi G, Zhang B, et al. Quantitative electroencephalogram in term neonates under different sleep states. *J Clin Monit Comput.* 2023;38:591–602. doi:10.1007/s10877-023-01082-6
36. Berry R, Quan S, Abreu A, Bibbs M. The AASM manual for the scoring of sleep and associated events. *Rul Terminol Techn Specific Dar Illin Am Acad Sleep Med.* 2012;176(2012):7.
37. Dubnov S. Generalization of spectral flatness measure for non-Gaussian linear processes. *IEEE Signal Process Lett.* 2004;11(8):698–701. doi:10.1109/LSP.2004.831663
38. Burns T, Rajan R. Combining complexity measures of EEG data: multiplying measures reveal previously hidden information. *F1000Res.* 2015;4:137. doi:10.12688/f1000research.6590.1
39. Hoban TF. Evolution of Sleep from Birth to Adolescence and Sleep Disorders in Children. In: Chokroverty S, editor. *Sleep Disorders Medicine: Basic Science, Technical Considerations and Clinical Aspects*. New York: Springer New York; 2017:1139–1158.
40. O’Reilly D, Navakatikyan MA, Filip M, Greene D, Van Marter LJ. Peak-to-peak amplitude in neonatal brain monitoring of premature infants. *Clin Neurophysiol.* 2012;123(11):2139–2153. doi:10.1016/j.clinph.2012.02.087
41. Whitehead K, Laudiano-Dray MP, Meek J, Fabrizi L. Emergence of mature cortical activity in wakefulness and sleep in healthy preterm and full-term infants. *Sleep.* 2018;41(8). doi:10.1093/sleep/zsy096

42. Corsi-Cabrera M, Cubero-Rego L, Ricardo-Garcell J, Harmony T. Week-by-week changes in sleep EEG in healthy full-term newborns. *Sleep*. 2020;43(4). doi:10.1093/sleep/zsz261
43. Paul K, Krajca V, Roth Z, Melichar J, Petránek S. Comparison of quantitative EEG characteristics of quiet and active sleep in newborns. *Sleep Med*. 2003;4(6):543–552. doi:10.1016/j.sleep.2003.08.008

Nature and Science of Sleep

Dovepress

Publish your work in this journal

Nature and Science of Sleep is an international, peer-reviewed, open access journal covering all aspects of sleep science and sleep medicine, including the neurophysiology and functions of sleep, the genetics of sleep, sleep and society, biological rhythms, dreaming, sleep disorders and therapy, and strategies to optimize healthy sleep. The manuscript management system is completely online and includes a very quick and fair peer-review system, which is all easy to use. Visit <http://www.dovepress.com/testimonials.php> to read real quotes from published authors.

Submit your manuscript here: <https://www.dovepress.com/nature-and-science-of-sleep-journal>